AFRL-ML-WP-TP-2004-407

(1 2 0) AND (1 2 2) MONAZITE DEFORMATION TWINS

R.S. Hay

Ceramics Branch (AFRL/MLLN)
Metals, Ceramics, and Nondestructive Evaluation Division
Materials and Manufacturing Directorate
Air Force Research Laboratory, Air Force Materiel Command
Wright-Patterson AFB, OH 45433-7750

June 2003

Approved for public release; distribution is unlimited.

STINFO FINAL REPORT

MATERIALS AND MANUFACTURING DIRECTORATE
AIR FORCE RESEARCH LABORATORY
AIR FORCE MATERIEL COMMAND
WRIGHT-PATTERSON AIR FORCE BASE, OH 45433-7750

NOTICE

Using government drawings, specifications, or other data included in this document for any purpose other than government procurement does not in any way obligate the U.S. Government. The fact that the government formulated or supplied the drawings, specifications, or other data does not license the holder or any other person or corporation; or convey any rights or permission to manufacture, use, or sell any patented invention that may relate to them.

This report has been reviewed by the AFRL Wright Site Office of Public Affairs (WS/PA) and is releasable to the National Technical Information Service (NTIS). At NTIS, it will be available to the general public, including foreign nationals.

This technical report has been reviewed and is approved for publication.

//s//

Pamela M. Schaefer
Principal Materials Engineer
Technical & Strategic Planning Office
Materials and Manufacturing Directorate

Copies of this report should not be returned unless return is required by security considerations, contractual obligations, or notice on a specific document.

REPORT DOCUMENTATION PAGE

Form Approved
OMB No. 0704-0188

1. REPORT DATE *(DD-MM-YY)*	2. REPORT TYPE	3. DATES COVERED *(From - To)*
June 2003	Journal article	

4. TITLE AND SUBTITLE
(1 2 0) AND (1 2 2) MONAZITE DEFORMATION TWINS

5a. CONTRACT NUMBER
IN-HOUSE

5b. GRANT NUMBER

5c. PROGRAM ELEMENT NUMBER
N/A

6. AUTHOR(S)
R.S. Hay

5d. PROJECT NUMBER
M05R

5e. TASK NUMBER
10

5f. WORK UNIT NUMBER
00

7. PERFORMING ORGANIZATION NAME(S) AND ADDRESS(ES)

Ceramics Branch (AFRL/MLLN)
Metals, Ceramics, and Nondestructive Evaluation Division
Materials and Manufacturing Directorate
Air Force Research Laboratory, Air Force Materiel Command
Wright-Patterson Air Force Base, OH 45433-7750

8. PERFORMING ORGANIZATION REPORT NUMBER
AFRL-ML-WP-TP-2004-407

9. SPONSORING/MONITORING AGENCY NAME(S) AND ADDRESS(ES)
Materials and Manufacturing Directorate
Air Force Research Laboratory
Air Force Materiel Command
Wright-Patterson Air Force Base, OH 45433-7750

10. SPONSORING/MONITORING AGENCY ACRONYM(S)
AFRL/MLLN

11. SPONSORING/MONITORING AGENCY REPORT NUMBER(S)
AFRL-ML-WP-TP-2004-407

12. DISTRIBUTION/AVAILABILITY STATEMENT
Approved for public release; distribution is unlimited.

13. SUPPLEMENTARY NOTES
Published in *Acta Materialia*, 51 (2003) 5255-5262. This material is declared a work of the U.S. Government and is not subject to copyright protection in the United States.

ABSTRACT ***(Maximum 200 Words),*** **,**
Unusual features of (1 2 0) and (1 2 2) deformation twins in monazite (monoclinic $LaPO_4$) are described and analyzed. These features are kinks and other irregularities in (1 2 0) twins, and V-shaped indentations on (1 2 0) and (1 2 2) twin planes. Twinning shear analysis suggests that the kinks area type II deformation twin mode with shear direction (η_1) of [2 1 0]. This complements previous analysis based on atom shuffling considerations. Shear strain compatibility requires extensive plastic deformation in the kink. The V-shaped indentions may be analogous to similar structures in b.c.c metal deformation twins. Deformation mechanisms that may be associated with these structures are discussed.

15. SUBJECT TERMS
Crystalline oxides, Transmission electron microscopy, Twinning, Modeling, Deformation structure

16. SECURITY CLASSIFICATION OF:			17. LIMITATION OF ABSTRACT:	18. NUMBER OF PAGES	19a. NAME OF RESPONSIBLE PERSON (Monitor)
a. REPORT	b. ABSTRACT	c. THIS PAGE			Randall S. Hay
Unclassified	Unclassified	Unclassified	SAR	12	19b. TELEPHONE NUMBER *(Include Area Code)* (937) 255-9825

Standard Form 298 (Rev. 8-98)
Prescribed by ANSI Std. Z39-18

Available online at www.sciencedirect.com
SCIENCE DIRECT®
Pergamon
Acta Materialia 51 (2003) 5255–5262
Acta MATERIALIA
www.actamat-journals.com

(1 2 0) and (1 2 $\bar{2}$) monazite deformation twins

R.S. Hay *

Air Force Research Laboratory, Materials and Manufacturing Directorate, WPAFB, OH, USA

Received 16 May 2003; received in revised form 27 May 2003; accepted 3 June 2003

Abstract

Unusual features of (1 2 0) and (1 2 $\bar{2}$) deformation twins in monazite (monoclinic $LaPO_4$) are described and analyzed. These features are kinks and other irregularities in (1 2 0) twins, and V-shaped indentations on (1 2 0) and (1 2 $\bar{2}$) twin planes. Twinning shear analysis suggests that the kinks are a type II deformation twin mode with shear direction (η_1) of [2 $\bar{1}$ 0]. This complements previous analysis based on atom shuffling considerations. Shear strain compatibility requires extensive plastic deformation in the kink. The V-shaped indentations may be analogous to similar structures in b.c.c metal deformation twins. Deformation mechanisms that may be associated with these structures are discussed. Published by Elsevier Ltd on behalf of Acta Materialia Inc.

Keywords: Crystalline oxides; Transmission electron microscopy; Twinning; Modeling; Deformation structure

1. Introduction

In a companion paper, five deformation twin planes were identified in monazite (monoclinic $LaPO_4$) indented at room temperature, and twin modes for these planes were suggested [1]. Conventions for description of these modes are given in that paper. It was suggested that the deformation twin modes in monazite tend to be those with the smallest atom shuffles and shuffling periodicity [1]. Two of these twins had unusual features. (1 2 0) twins were kinked on the '(4 8 3)' plane, and in some cases appeared to be resorbed by the parent grain. Both (1 2 0) and (1 2 $\bar{2}$) twins had V-shaped indentations [1]. Thorough description and analysis of these twins and their unusual features is the subject of this paper. The likely modes for these twins were identified as $(1\,2\,0)[0\,1\,0]_I$, $(1\,2\,\bar{2})\ [0\,1\,\bar{1}]_I$, and the kink in (1 2 0) twins was suggested to be $(1\,0\,0)[2\,1\,0]_{II}$ [1]. Analysis that supports these mode identifications is presented here. Analogues to features of deformation twinning in b.c.c. metals are also discussed [2,3].

Monazite ($LaPO_4$) is refractory (mp 2072 °C), relatively soft (5 GPa), and machinable [4,5]. It is stable with many common structural oxide ceramics [6]. The weakness of monazite relative to other refractory oxides in both the brittle and ductile field makes it interesting for various structural applications [4,5,7–13]. As before [1], we use the $P2_1/n$ monoclinic space group convention to describe monazite, with lattice parameters a = 0.6825 nm, b = 0.7057 nm, c = 0.6482 nm, and β = 103.21°.

* Tel.: +1-937-2559825; fax: +1-937-6564296.
E-mail address: Randall.Hay@wpafb.af.mil (R.S. Hay).

1359-6454/$30.00 Published by Elsevier Ltd on behalf of Acta Materialia Inc.
doi:10.1016/S1359-6454(03)00304-5

AS-03-1224

RG 5.1

2. Experiments

Monazite powder was hot-pressed to a 5–20 μm grain size. The hot-pressed material was indented at room temperature with 20 kg load and a 3 mm spherical tungsten carbide indenter [1,4]. TEM samples of regions underneath the indents were prepared as previously described [14–16]. TEM observations were done in a Phillips CM200 TEM with a field emission gun operating at 200 kV. TEM negatives were digitized and measurements were made off the digital images. Further details are given in a companion paper [1].

3. Results and discussion

3.1. General

Five out of a total of seventy observed twins were (1 2 0) twins. They were observed along [0 0 1], [2 $\bar{1}$ 1], [2 $\bar{1}$ 0], and [4 $\bar{2}$ 3] zones (Fig. 1). They averaged 28 nm in width. One was cracked on one side, showing (1 2 0) cleavage. Grains containing these twins had either no evidence of dislocation slip, or low dislocation densities. (1 2 0) twins have a close match with a low Σ CSL, which suggests they may have low interface energy [1]. The atomic shuffle displacements and shuffling periodicity for the (1 2 0)[0 1 0]$_I$ mode are the smallest of all the possible (1 2 0) modes with index ≤4. The presence of a reflection plane across the (1 2 0) twin plane rules out a type II mode that also has small shuffle displacements and periodicity, so (1 2 0)[0 1 0]$_I$ was suggested to be the operating mode [1].

3.2. Indentations

One (1 2 0) twin had a V-shaped indentation defined by (1 2 $\bar{2}$) and (1 2 2) (Fig. 2). Since the sides of the indentation show little or no projection on the [2 $\bar{1}$ 0] imaging zone, the indentation must be aligned with [2 $\bar{1}$ 0], and therefore fairly well aligned with the shear direction η_1 for this twin mode, which is '[4 $\bar{2}$ 1]'.

Twin boundaries with indentations that are aligned with η_1 are found in deformation twins in b.c.c. metals [2]. A suggested formation mechanism involves hindrance of twinning screw dislocations by an obstacle during lateral twin growth. The twinning dislocations combine to form lattice dislocations, which move around the obstacle by cross slip, forming the

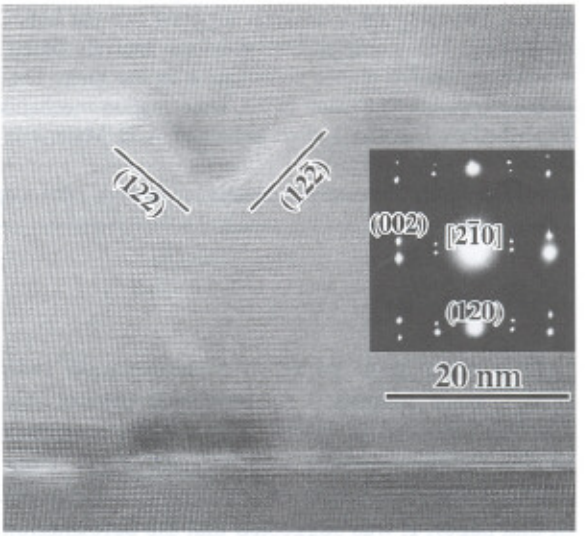

Fig. 2. Indented (1 2 0) twin. The sides of the indent are (1 2 $\bar{2}$) and (1 2 2) planes of the twin lamellae.

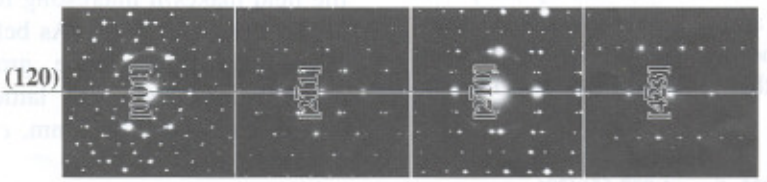

Fig. 1. Electron diffraction patterns for the (1 2 0) twin along four different zones.

indentation (Fig. 3) [2]. The twinning shear direction η_1, twinning dislocation b_T, and lattice dislocation b_L must all have the same direction, and for b.c.c. metals this is [1 1 $\bar{1}$] (Fig. 3).

Despite dissimilarity in the materials systems, indents in (1 2 0) monazite twins resemble those in (1 1 2) b.c.c. metal twins. The morphology is similar, and in both cases the indent axis appears to be aligned with the twin shear direction (η_1). We examine whether the suggested b.c.c. metal indentation formation mechanism can apply to monoclinic $LaPO_4$.

The twinning dislocations ($\mathbf{b_T}$) for the (1 2 0) twin are [17]:

$$\mathbf{b}_{\mathbf{T}(1\ 2\ 0)} = ds\eta_{1\hat{n}} \approx 0.33'[4\ \bar{2}\ 1]'_{\hat{n}}\ (\mathrm{nm}) \qquad (1)$$

where d is the (1 2 0) plane spacing, s is the twin shear, and $\eta_{1\hat{n}}$ is a unit vector along η_1. In b.c.c. crystals, the twinning and slip directions are the same. For type I twins in a monoclinic material like monazite, η_1 is irrational (in this case very close to [4 $\bar{2}$ 1]), and cannot be a lattice dislocation Burgers vector. Also, η_1 of $'[4\ \bar{2}\ 1]'$ is not exactly cozonal with (1 2 2) and (1 2 $\bar{2}$), but it is close. Within about 1% error:

$$\mathbf{b}_{\mathbf{T}(1\ 2\ 0)} \approx \frac{2}{9}[2\ \bar{1}\ 0] + \frac{1}{10}[0\ 0\ 1] \qquad (2)$$

[2 $\bar{1}$ 0] dislocations can glide on (1 2 0), (1 2 2) or (1 2 $\bar{2}$); [0 0 1] dislocations can glide on (1 2 0). The [2 $\bar{1}$ 0] dislocation size of 1.54 nm would seem to prohibit its existence unless it dissociates. It is unclear how the relatively small number of [0 0 1] dislocations would bypass obstacles. If η_1 was misidentified and was actually [2 $\bar{1}$ 0], the [0 0 1] component would be unnecessary, but clearly this cannot be true—the twin was imaged along the [2 $\bar{1}$ 0] zone, and misorientation across the boundary is clear in electron diffraction patterns and lattice images (Fig. 2).

Poorly developed indentations were also observed on (1 2 $\bar{2}$) twin boundaries (Fig. 4). The indentations were weakly defined by (0 0 1) and (1 2 0). The mode for this twin was identified as (1 2 $\bar{2}$) [0 1 $\bar{1}$]$_I$ [1]. Here η_1 is $'[9\ \bar{4}\ 0]'$, which, like the (1 2 0) indentation, is also close to [2 $\bar{1}$ 0]. By analysis similar to Eqs. (1) and (2):

$$\mathbf{b}_{\mathbf{T}(1\ 2\ \bar{2})} \approx 0.096'[9\ \bar{4}\ 0]'_{\hat{n}}\ (\mathrm{nm}) \approx \frac{1}{16}[2\ \bar{1}\ 0] + \frac{\sim 1}{50}[1\ 0\ 0] + \frac{\sim 1}{100}[0\ 0\ 1] \qquad (3)$$

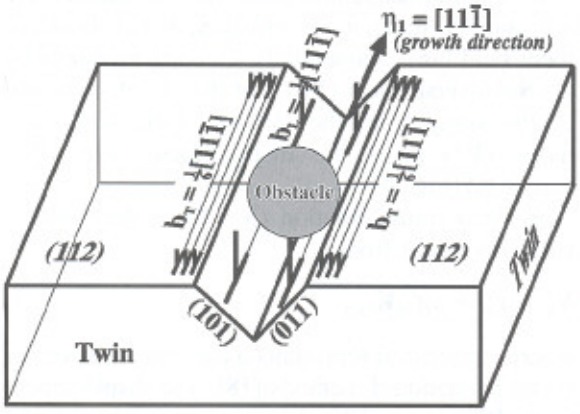

Fig. 3. Schematic of indentation formation during twinning in b.c.c. metals (after Narita and Takamura).

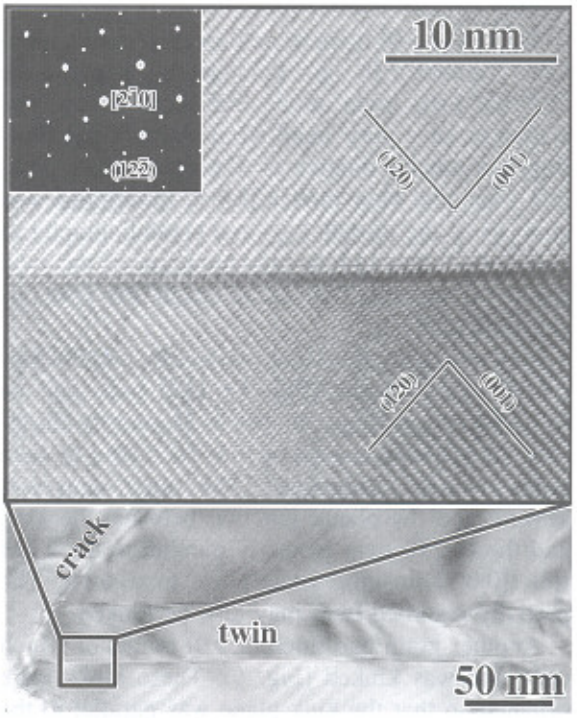

Fig. 4. Indentation in a (1 2 $\bar{2}$) twin (upper twin boundary, right hand side). This twin terminates at a (0 0 1) cleavage crack.

As with the (1 2 0) indentation, [2 $\bar{1}$ 0] dislocations can glide on the (1 2 $\bar{2}$) twin plane as well as the (0 0 1) and (1 2 0) indentation planes. However, it is also unclear how the small number of [1 0 0] and [0 0 1] dislocations would bypass obstacles.

For both (1 2 0) and (1 2 $\bar{2}$) twins, the indentation axis lies along η_1 (which in both cases is close to [2 $\bar{1}$ 0]), as it also does for b.c.c. metals [2]. However, unlike b.c.c. metals, formation of the indentations requires formation of large [2 $\bar{1}$ 0] lattice dislocations from twinning dislocations, dissociation of these lattice dislocations, cross-slip of these dissociated dislocations along the indentation planes, and possibly minor glide through growth obstacles by other dislocations along the twin plane. Independent evidence of [2 $\bar{1}$ 0] monazite dislocations, or their equivalent, that slip on (1 2 2), (1 2 $\bar{2}$), (1 2 0), and (0 0 1) is necessary to confirm the analogy with b.c.c. metals.

3.3. Kinks

Kinked (1 2 0) twins were observed in two monazite grains. In a companion paper, the (1 0 0)[2 1 0]$_{II}$ twin mode for these kinks was shown to have very small atom shuffles and shuffling periodicity relative to almost all other possible monazite twin modes [1]. A description and analysis of the morphology and crystallography of the kinks follows, with determination of the twin mode by methods that complement the previous shuffling analysis.

One monazite grain had two nearly parallel lenticular (1 2 0) twins (Fig. 5). One twin had an irregular morphology; in places it entirely disappears, suggesting resorption into the matrix by twin grain boundary migration. The other twin was kinked, and the planar junction between the kink and the (1 2 0) twin is nearly parallel to the TEM foil ([0 0 1] imaging zone, close to (0 0 1)). The partially resorbed twin may also be kinked.

Another grain had three (1 2 0) twins, of which only one was kinked (Fig. 6). These kinks were oriented so that the kink plane was parallel to the [2 $\bar{1}$ 0] imaging zone. In this orientation the kink can be identified. The twin–matrix, kink–matrix, and kink–twin planes ($\mathbf{K_1}$) are denoted by superscripts A, B, and C, respectively (Fig. 6). $\mathbf{K_1^A}$ is (1 2 0). $\mathbf{K_1^C}$ the planar junction between the kink and the (1 2 0) twin, is misoriented about 6° from (0 0 1), similar to the orientation of the same junction in Fig. 5. Although there is some variation of the $\mathbf{K_1^B}$ plane orientation in different kinks, by inspection from Fig. 6, $\mathbf{K_1^B}$ is close to (1 2 1). Although variable in intensity, probably because of the sample thickness and difficulty in tilting exactly to the [2 $\bar{1}$ 0] zone, the (0 0 1) planes are not misoriented across $\mathbf{K_1^B}$. Therefore $\mathbf{K_1^B}$ cannot be a plane of reflection, and the [2 $\bar{1}$ 0] zone axis must be coincident with η_1^B where the (0 0 1) planes are related by a 180° rotation around [2 $\bar{1}$ 0] rather than a reflection across $\mathbf{K_1^B}$. The "B" twin is therefore a type II twin with η_1^B(shear direction) of [2 $\bar{1}$ 0]. This is close to the shear direction of the (1 2 0) "A" twin (η_1^A = '[4 $\bar{2}$ 1]').

From $\mathbf{K_1^B}$ of ~(1 2 1) and η_1^B of [2 $\bar{1}$ 0], the plane of shear that contains K_1, K_2, η_1, and η_2 for the "B" twin can be found from a stereonet (Fig. 7). To minimize the displacement field across $\mathbf{K_1^C}$, we assume that the shear (s) of the B twin is similar to that of the (1 2 0) twin (s = 1.06). Only one possibility with indices ≤2 is evident—a (1 0 0)[2 $\bar{1}$ 0]$_{II}$ mode with shuffling periodicity (λ) of 1 ($\mathbf{K_1^B}$ = '(4 8 3)', s = 1.16). A (1 2 1)[0 2 1]$_{II}$ mode with shuffling periodicity (λ) of 5 (s = 1.17) has a similar shear transformation, but besides having high shuffling periodicity it requires reflection across $\mathbf{K_1^B}$, rather than the observed 180° rotation (Figs. 6 and 7).

In general, sequential shear transformations are not another shear transformation, but a displacement field [18]. Sequentially shearing monazite by (1) the inverse shear $(\mathbf{V^A})^{-1}$ of the (1 2 0) twin and 2) the shear from the ($\bar{1}$ 0 0)[$\bar{2}$ 1 0]$_{II}$ kink twin mode ($\boldsymbol{V^B}$) gives the displacement field ($\boldsymbol{W^C}$) across $\mathbf{K_1^C}$(Fig. 6).

A shear transformation ($\underline{\mathbf{V}}_k^i$) for a deformation twin can found from:

$$\mathbf{V}_k^i = \delta_k^i + s\eta_{1\tilde{\mathbf{n}}}^i \mathbf{K}_{1k\tilde{\mathbf{n}}} \tag{4}$$

where subscript $\tilde{\mathbf{n}}$ represents a cartesian unit vector found by standard methods [18]. The displacement field ($\boldsymbol{W^C}$) across $\mathbf{K_1^C}$ is:

$$\boldsymbol{W^C} = (\boldsymbol{V^A})^{-1} \times \boldsymbol{V^B} \tag{5}$$

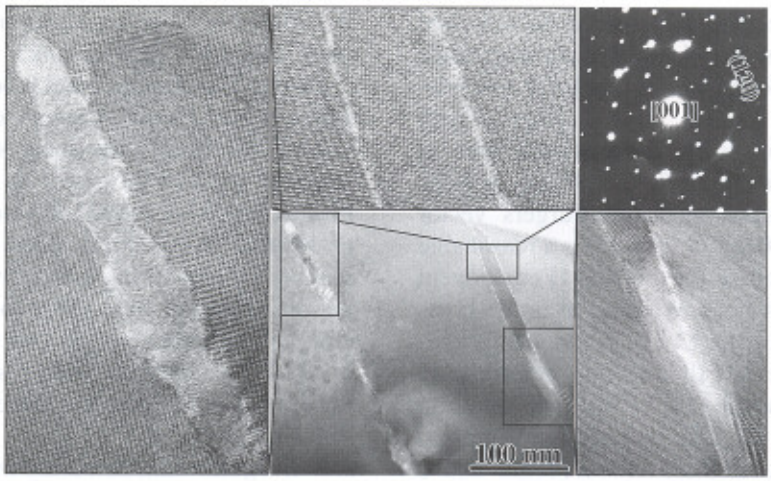

Fig. 5. Parallel (1 2 0) twins. The twin on the left has irregular morphology and looks like it has been resorbed into the matrix. The twin on the right is kinked on a plane almost parallel to the TEM foil.

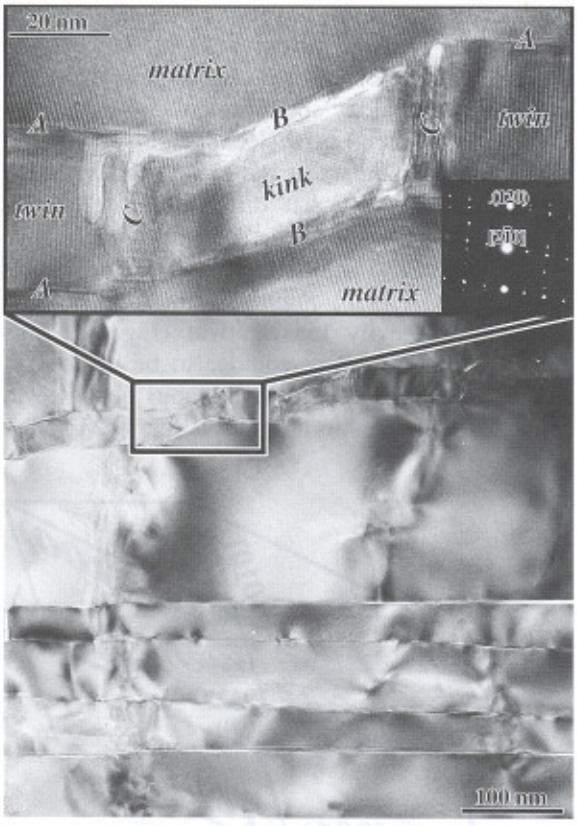

Fig. 6. Kinked (1 2 0) twins, viewed along the [2 $\bar{1}$ 0] imaging zone. The kink lies along '(4 8 3)' and there is no rotation of (0 0 1) lattice fringes across '(4 8 3)'.

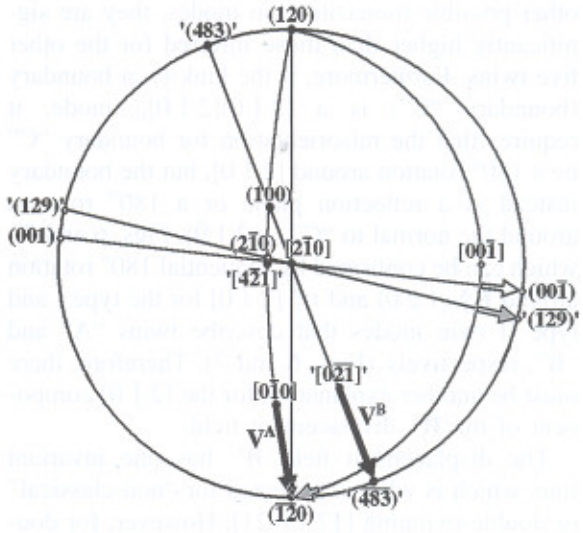

Fig. 7. Stereonet showing principal directions and planes of shear for twin modes for the (1 2 0) twin and the '(4 8 3)' kink, and the slip systems that must be active to accommodate deformation in the kink. Solid arrows show twin shears (η_2 to K_1); gray arrows show shears necessary to accommodate compatibility strain, and white arrows show how shear on '(1 2 9)' can be decomposed to shear on (0 0 1) and (1 2 0). The stereonet is drawn with the same orientation as the TEM image in Fig. 6.

$\boldsymbol{W}^C$ has one eigenvector very close to $[2\ \bar{1}\ 0]_{crystal}$. Therefore $\boldsymbol{W}^C$ is a displacement field with an invariant line, rather than a shear transformation, which would have an invariant plane with two

orthogonal eigenvectors. $\boldsymbol{W}^{C}$ can be decomposed into two shear transformations of shear magnitude s and direction η along plane K ($s[\eta](K)$), one with 0.220[0 0 $\bar{1}$](1 2 0), and the other with 0.424[2 $\bar{1}$ 0]'(1 2 9)', where the irrational plane is more accurately given as (0.053, 0.105, 0.993). [0 0 1] is the smallest monazite Burgers vector (0.65 nm) [16], so [0 0 1](1 2 0) slip is a reasonable deformation mechanism for the [0 0 1] component of the displacement field. We next examine possible explanations for the [2 $\bar{1}$ 0] component.

The shear in the [2 $\bar{1}$ 0] direction is extremely close to that for the (2 $\bar{1}$ 0)[2 $\bar{1}$ 0]$_{II}$ twin mode (s = 0.426, K_1 = '(1 2 9)', Fig. 7). Maximum La atom and PO_4 tetrahedra shuffles of ~0.14 nm and a shuffling periodicity λ of 5 were found for this mode by methods discussed previously [1]. Although the shuffles are small compared to most other possible monazite twin modes, they are significantly higher than those inferred for the other five twins. Furthermore, if the kink-twin boundary (boundary "C") is a (2 $\bar{1}$ 0)[2 $\bar{1}$ 0]$_{II}$ mode, it requires that the misorientation for boundary "C" be a 180° rotation around [2 $\bar{1}$ 0], but the boundary instead is a reflection plane or a 180° rotation around the normal to "C" (~[$\bar{2}$ 1 $\bar{9}$], Figs. 6 and 7), which can be confirmed by sequential 180° rotation around $\mathbf{K}_1^{A}$ (1 2 0) and η_1^{B} [2 $\bar{1}$ 0] for the type I and type II twin modes that describe twins "A" and "B", respectively (Figs. 6 and 7). Therefore, there must be another explanation for the [2 $\bar{1}$ 0] component of the $\boldsymbol{W}^{C}$ displacement field.

The displacement field $\boldsymbol{W}^{C}$ has one invariant line, which is what is expected for "non-classical" or double-twinning [17,19–21]. However, for double-twinning the invariant line of the displacement field is perpendicular to the shear direction for both twins, but for $\boldsymbol{W}^{C}$ the [2 $\bar{1}$ 0] invariant line is coincident to the shear direction. Therefore a double-twinning mechanism cannot explain the [2 $\bar{1}$ 0] component of $\boldsymbol{W}^{C}$.

The 0.424[2 $\bar{1}$ 0]'(1 2 9)' shear can be decomposed to shear on rational planes: 0.417[2 $\bar{1}$ 0](0 0 1) and 0.045[2 $\bar{1}$ 0](1 2 0) (Fig. 7). These are the same slip planes and directions inferred for growth of indentations on (1 2 $\bar{2}$) twin planes (Section 3.2). The [0 0 1](1 2 0), [2 $\bar{1}$ 0](0 0 1), and [2 $\bar{1}$ 0](1 2 0) slip systems are therefore suggested to accommodate the displacement field ($\boldsymbol{W}^{C}$) for the kink.

Precise calculations cannot be made because the single crystal elastic constants of monazite are not known, but clearly the shear stress from a shear strain of >0.4 (>20°) is of at least 10 GPa level. Presumably, kink formation would be energetically prohibitive if this stress were not simultaneously relieved by slip during kink growth. Topologically, the displacement field ($\boldsymbol{W}^{C}$) for the kink requires emission of approximately one **b** = [0 0 1] and one **b** = [2 $\bar{1}$ 0] dislocation (or its dissociated equivalent) for every 10 (1 2 0) layers at the kink growth front.

3.4. Irregular kink-boundary morphology

It was previously noted that kink boundary ("B") orientations varied from kink to kink (Fig. 6), and that some (1 2 0) twins have highly irregular boundaries that suggests they are heavily kinked, or resorbed into the parent grain by some other process (Fig. 5). Several explanations for the irregular morphology seem possible.

In one grain (Fig. 6), dislocation slip systems in the parent grain intersect the kinked twins, which may contribute to local distortion of the twin boundaries. The prevalence of kinks might also affect boundary morphology—the "resorbed" (1 2 0) twin (Fig. 5) might be an example of a particularly heavily kinked twin (Fig. 8). This "resorbed" morphology could also be an artifact from a 2-D slice through a continuous twin growth front that undulates in and out of the TEM foil.

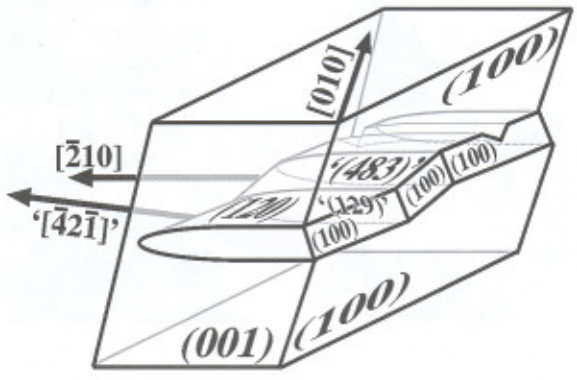

Fig. 8. Schematic diagram of kinked twins.

The irregular morphology could be intrinsic to the extensive dislocation emission required during kink growth. Variations in morphology could be related to local hindrance of dislocation emission and motion. This would generate very high stress that could drive strain induced boundary migration of the twin boundaries. In the TEM image of Fig. 6 there may be voids along kink ("B") and kink-twin boundaries ("C") that could form from such stress. It is not clear how thermally activated processes such as void growth and boundary migration could take place during room temperature indentation in a refractory material like monazite. However, microstructures resembling dynamic recrystallization have been observed in monazite coatings on fibers during fiber push-out at room temperature [22], and monazite can recrystallize at near-room temperature after radiation damage [22–25].

4. Summary and conclusions

Deformation twins on (1 2 0) and (1 2 $\bar{2}$) form occasionally in monazite. Both twins have indentations with an axis that is very close to [2 $\bar{1}$ 0], which is also very close to the respective twin shear directions (η_1) of '[4 $\bar{2}$ 1]' and '[9 $\bar{4}$ 0]'. These indentations are similar to those observed in b.c.c. metals. If the formation mechanisms are analogous to b.c.c. metals, [2 $\bar{1}$ 0] screw dislocations that presumably dissociate form from twinning dislocations in monazite during indentation formation.

(1 2 0) twins are occasionally kinked on '(4 8 3)'. From the crystallography of the kink inferred from TEM lattice images, and analysis of shear strain during twinning, the kink twin mode can be deduced to be (1 0 0)[2 $\bar{1}$ 0]$_{II}$. This analysis complements the mode determination done by analysis of atomic shuffling presented in a companion paper [1]. It is not clear why (1 0 0)[2 1 0]$_{II}$ deformation twins occur only as kinks in (1 2 0)[0 1 0]$_{I}$ deformation twins, or why they occur in some (1 2 0) twins and not others, even in the same grain.

Shear strain compatibility requires extensive plastic deformation during kink formation. The [2 1 0](0 0 1), [2 1 0](1 2 0), and [0 0 1](1 2 0) slip systems are required for this deformation. As for boundary indentations, [2 1 0] dislocations presumably dissociate. It will be interesting to see if these [2 $\bar{1}$ 0] slip systems, or their dissociated equivalents, can be independently observed. Irregularities in boundary morphology of (1 2 0) twins and their kinks may be related to hindrance of dislocation slip, but other explanations are possible.

Acknowledgements

P. Hazzeldine directed the author to the literature on indentations in b.c.c. metal twins. J. B. Davis supplied the indented monazite. D. B. Marshall had many valuable suggestions. This work was supported by the Air Force Office of Scientific Research.

References

[1] Hay RS, and Marshall DB, Monazite Deformation Twins. Acta mater.
[2] Narita N, Takamura J. Deformation twinning in f.c.c. and b.c.c. metals. In: Nabarro FRN, editor. Dislocations in solids. Elsevier Science; 1992. p. 135–89.
[3] Yoo MH. Deformation twinning in superlattice structures. J. Mater. Res. 1989;4(1):50–4.
[4] Davis JB, Marshall DB, Housley RM, Morgan PED. Machinable ceramics containing rare-earth phosphates. J. Am. Ceram. Soc. 1998;81(8):2169–75.
[5] Morgan PED, Marshall DB. Ceramic composites of monazite and alumina. J. Am. Ceram. Soc. 1995;78(6):1553–63.
[6] Marshall DB, Morgan PED, Housley RM, Cheung JT. High-temperature stability of the Al_2O_3–$LaPO_4$ system. J. Am. Ceram. Soc. 1998;81(4):951–6.
[7] Davis JB, Marshall DB, Morgan PED. Oxide composites of $LaPO_4$ and Al_2O_3. J. Eur. Ceram. Soc. 1999;19:2421–6.
[8] Davis JB, Marshall DB, Morgan PED. Monazite containing oxide–oxide composites. J. Eur. Ceram. Soc. 2000;20(5):583–7.
[9] Keller KA. Evaluation of all-oxide composites based on coated Nextel™ 610 and 650 fibers. Cer. Eng. Sci. Proc. 2001;22(3):667–75.
[10] Johnson SM, Blum Y, Kanazawa C, Wu H-J, Porter JR, Morgan PED et al. Processing and properties of an oxide/oxide composite. Key Eng. Mater. 1997;127-131:231–8.
[11] Johnson SM, Blum Y, Kanazawa C, Wu H-J. Low-cost matrix development for an oxide–oxide composite. Met. Mater. 1998;4(6):1119–25.

[12] Keller KA, Parthasarathy TA, Mah T, Boakye E. Evaluation of monazite fiber coatings in dense matrix composites. Ceram. Eng. Sci. Proc. 1999;20(3):451–61.
[13] Keller KA, Mah T, Boakye EE, Parthasarathy TA. Gel-casting and reaction bonding of oxide–oxide minicomposites with monazite interphase. Cer. Eng. Sci. Proc. 2000;21(3):525–34.
[14] Hay RS, Welch JR, Cinibulk MK. TEM specimen preparation and characterization of ceramic coatings on fiber tows. Thin Solid Films 1997;308-309:389–92.
[15] Cinibulk MK, Welch JR, Hay RS. Preparation of thin sections of coated fibers for characterization by transmission electron microscopy. J. Am. Ceram. Soc. 1996;79(9):2481–4.
[16] Hay RS. Monazite and scheelite deformation mechanisms. Cer. Eng. Sci. Proc. 2000;21(4):203–18.
[17] Christian JW, Mahajan S. Deformation twinning. Prog. Mat. Sci. 1995;39(1/2):1–157.
[18] Bollmann W. Crystal lattices, interfaces, matrices. 1st ed. Published by the Author. 1982. p. 360.
[19] Bevis M, Crocker AG. Twinning shears in lattices. Proc. Roy. Soc. 1968;A304:123–34.
[20] Bevis M, Crocker AG. Twinning modes in lattices. Proc. Roy. Soc. 1969;A313:509–29.
[21] Crocker AG, Abell JS. The crystallography of deformation kinking. Phil. Mag. 1976;33(2):305–10.
[22] Davis JB, Hay RS, Marshall DB, Morgan PED, Sayir A. The Influence of Interfacial Roughness on Fiber Sliding in Oxide Composites with La-Monazite Interphases. J Am Ceram Soc 2003;86(2):305–16.
[23] Karioris FG, Gowda KA, Cartz L. Heavy ion bombardment of monoclinic $ThSiO_4$, ThO_2, and monazite. Rad. Eff. Lett. 1981;58:1–3.
[24] Ehlert TC, Gowda KA, Karioris FG, Cartz L. Differential scanning calorimetry of heavy ion bombarded synthetic monazite. Rad. Eff. 1983;70:173–81.
[25] Meldrum A, Boatner LA, Ewing RC. A comparison of radiation effects in crystalline ABO4-type phosphates and silicates. Mineral. Mag. 2000;64(2):185–94.